Letter

Distance between various discretized fermion actions

Dian-Jun Zhao,[1,2] Gen Wang,[3,4] Fangcheng He,[2] Luchang Jin,[5,6] Peng Sun,[7]
Yi-Bo Yang,[1,2,8,9] and Kuan Zhang[1,2]

(χQCD Collaboration)

[1]*University of Chinese Academy of Sciences, School of Physical Sciences, Beijing 100049, China*
[2]*CAS Key Laboratory of Theoretical Physics, Institute of Theoretical Physics, Chinese Academy of Sciences, Beijing 100190, China*
[3]*Department of Physics and Astronomy, University of Kentucky, Lexington, Kentucky 40506, USA*
[4]*Aix-Marseille Universit, Universit de Toulon, CNRS, CPT, UMR 7332 Marseille, France*
[5]*Physics Department, University of Connecticut, Storrs, Connecticut 06269, USA*
[6]*RIKEN-BNL Research Center, Brookhaven National Laboratory, Upton, New York 11973, USA*
[7]*Institute of Modern Physics, Chinese Academy of Sciences, Lanzhou 730000, China*
[8]*School of Fundamental Physics and Mathematical Sciences, UCAS, Hangzhou 310024, China*
[9]*International Centre for Theoretical Physics Asia-Pacific, Beijing/Hangzhou, China*

(Received 3 August 2022; accepted 3 April 2023; published 1 May 2023)

We present the leading-order mixed-action effect $\Delta_{\mathrm{mix}} \equiv m^2_{\pi,\mathrm{vs}} - \frac{m^2_{\pi,\mathrm{vv}}+m^2_{\pi,\mathrm{ss}}}{2}$ using highly improved staggered quarks (HISQ), clover, or overlap valence fermion actions on gauge ensembles using various sea fermion actions across a widely used lattice spacing range $a \in [0.04, 0.19]$ fm. The results suggest that Δ_{mix} decreases as the fourth order of the lattice spacing on the gauge ensembles with dynamical chiral sea fermions, such as domain wall or HISQ fermions. When a clover sea fermion action that has explicit chiral symmetry breaking is used in the ensemble, Δ_{mix} can be much larger regardless of the valence fermion action used.

DOI: 10.1103/PhysRevD.107.L091501

I. INTRODUCTION

Lattice provides a unique gauge invariant, nonperturbative regularization method for non-Abelian gauge field theories. However, the infamous fermion doubling problem prevents a straightforward discretization of the continuum Dirac fermion action used in four-dimensional lattice QCD calculations. The overlap (OV) fermion [1–3], which satisfies the Ginsparg-Wilson relation, would be the optimal choice for the discretized Dirac operator, but requires a factor of $\mathcal{O}(100)$ cost of computational resources compared to the widely used Wilson-like fermions; on the other hand, the staggered fermion and its improved versions can also provide exact chiral symmetry with a cost much lower than the Wilson-like fermion, at the expense of mixing between four equivalent "tastes" of a given flavor. Ideally, results obtained with different fermion formulations are expected to agree in the continuum limit. But for practical lattice spacings used in the state-of-the-art lattice calculations, it is not entirely clear to what extent they should agree [4].

Since, in practice, generating large ensembles using an expensive fermion action can take several months or even years, using a more expensive "valence" fermion action on an ensemble generated with a cheaper "sea" fermion action has become a popular compromise in the past decade, such as in the calculations of the glue helicity [5], nucleon axial charge [6,7], hadron vacuum polarization [8], and so on. But most of the conventional lattice QCD studies still prefer a single fermion action for both the valence and sea fermions, as the "mixed-action" setup can introduce additional discretization effects as well as those (e.g., Ref. [9]) from the valence and sea fermions themselves.

From the analytical side, the mixed-action partially quenched chiral perturbation theory (MAPQχPT) [10–12] suggests that the only mixed-action effect at leading order is replacing the mass squared $m^2_{\pi,\mathrm{vs}}$ of "mixed-action pion" with one valence quark and one sea antiquark into $m^2_{\pi,\mathrm{vs}} = \frac{m^2_{\pi,\mathrm{vv}}+m^2_{\pi,\mathrm{ss}}}{2} + \Delta^{\mathrm{B/A}}_{\mathrm{mix}}(a)$, where $m_{\pi,\mathrm{vv}}$ is the pion mass with two valence quarks of action A, and $m_{\pi,\mathrm{ss}}$ is that with two sea quarks of action B. After this replacement, standard

Published by the American Physical Society under the terms of the Creative Commons Attribution 4.0 International license. Further distribution of this work must maintain attribution to the author(s) and the published article's title, journal citation, and DOI. Funded by SCOAP[3].

partially quenched (PQ) χPT can be applied to study nucleon twist-two matrix elements, the nucleon-nucleon system, neutron electric dipole moment, and so on [12]. Recent high-precision mixed-action lattice QCD studies with different pion masses also show that the pion form factor (which is related to the rho meson pole) can be described by PQχPT if and only if the above mixed-action replacement is applied [13]. Thus, we can define an additional leading-order MAPQχPT low-energy constant as

$$\Delta_{\rm mix}^{\rm B/A}(m_{\pi,\rm vv}, m_{\pi,\rm ss}, a) \equiv m_{\pi,\rm vs}^2 - \frac{m_{\pi,\rm vv}^2 + m_{\pi,\rm ss}^2}{2}, \quad (1)$$

and it is generally assumed that $\Delta_{\rm mix}^{\rm B/A}$ is a $\mathcal{O}(a^2)$ effect in most of the cases.

On the other hand, the numerical lattice QCD studies are very limited in number. Assuming $m_{\pi,\rm vv} = m_{\pi,\rm ss} \sim 300$ MeV and $a \sim 0.09$ fm, the mixed-action effect will make $\delta m_\pi \equiv m_{\pi,\rm vs} - m_{\pi,\rm ss}$ to be 153(59) MeV for the overlap valence quark on the clover (CL, a typical Wilson-like fermion) sea [14], while δm_π will be reduced to 30–60 MeV for the combination of the domain wall fermion (DW, a different implementation of the overlap fermion by introducing an extra fifth dimension for the fermion) valence and staggered sea [15–17], and it can be as small as $\sim$10 MeV if we use the overlap valence quark on the DW sea [18]. There are also studies on other combinations, such as overlap on highly improved staggered quarks (HISQ) [19] at $a \simeq 0.12$ fm [20].

However, all of the above estimates, which are based on the imprecise calculation at $a \sim 0.1$ fm, can misrepresent the situation and render the reliability of any high-precision mixed-action calculation questionable. In this work, we present the most systematic mixed-action-effect study so far with several valence and sea fermion combinations. The results suggest that $\Delta_{\rm mix}$ decreases faster than the naive a^2 estimate in all the cases we studied and at $\mathcal{O}(a^4)$ when the fermion action used in the sea has chiral symmetry.

II. METHODOLOGY AND SETUP

The naive fermion action has the infamous fermion doubling problem, and it leads to 16 fermions as opposed to one in four dimensions. The staggered fermion introduces a redefinition of the quark field [e.g., $\psi_{\rm st}(x) = \gamma_4^{x_4}\gamma_1^{x_1}\gamma_2^{x_2}\gamma_3^{x_3}\psi(x)$ at the site $x = \{x_1, x_2, x_3, x_4\}$ in the MILC convention] to partially fix the fermion doubling problem, and further improvement such as the use of the HISQ action [19] is needed to suppress the mixing between the four residual fermions. On the other hand, the Wilson fermion avoids the entire doubling problem, but it introduces an explicit chiral symmetry breaking effect on the quark mass. Such an effect can be suppressed by adding a clover term. The solution to avoid the entire fermion doubling problem without explicit chiral symmetry breaking is to use a Ginsparg-Wilson action [21], such as the overlap fermion [22,23]. More details of the fermion actions can be found in the Supplemental Material [24].

At the next-to-leading order (NLO) of the PQχPT, the mixed-action effect defined in Eq. (1) can be nonzero when $m_{\pi,\rm vv} \neq m_{\pi,\rm ss}$, even if the fermion actions used by the valence and sea quarks are the same. Thus, in this work, we majorly concentrate on the unitary case with the valence pion mass tuned to be the same as the sea pion mass,

$$\Delta_{\rm mix,uni}(m_\pi, a) \equiv \Delta_{\rm mix}(m_\pi, m_\pi, a). \quad (2)$$

$\Delta_{\rm mix,uni}$ approaches exactly zero in the continuum and thus is a good reference to verify the additional discretization error in the mixed fermion action simulation. Such a definition is different from that used in the previous χQCD study [18], but still provides consistent results, and detailed comparisons can be found in the Supplemental Material [24].

Since the Hypercubic (HYP) smearing [25] can make the cost of the overlap fermion calculation to be much cheaper and the fluctuation of the clover fermion around the physical pion mass to be smaller, we will concentrate on the following three kinds of the valence fermion actions to calculate $\Delta_{\rm mix}$:

(1) *OV*: Overlap fermion with one-step HYP smearing and $\rho = 1.5$.
(2) *HI*: HISQ action without any additional smearing on the gauge link.
(3) *CL*: Clover fermion with one-step HYP smearing and tree level tadpole improved clover coefficient $c_{sw} = \langle U_p\rangle^{-3/4}$, where $\langle U_p\rangle$ is the vacuum expectation value of the plaquette on the HYP smeared configurations, calculated nonperturbatively on each gauge ensemble.

For the sea fermion actions, we use three kinds of the gauge ensembles to cover the popular choices:

(1) those from the RBC/UKQCD Collaboration, which use the 2 + 1 flavor DW fermion action and Iwasaki gauge action (I) at four lattice spacings and physical pion mass [26,27], noting that the ensembles at the two largest lattice spacings include the dislocation suppressing determinant ratio (DSDR) term [27] (DW + Iwasaki + DSDR, DD for short) and those at the finer two lattice spacings do not (DW + I, DW for short);
(2) those from the MILC Collaboration, which use the 2 + 1 + 1 flavor HISQ fermion action with one-loop Symanzik improved gauge action [28] at four lattice spacings and $m_\pi = 310$ MeV [29–31] (HI + S$^{(1)}$, HI for short); and
(3) those from the CLQCD Collaboration, which use the 2 + 1 flavor tadpole improved clover fermion action (with one-step stout link smearing on

TABLE I. Information of the ensembles [26,27,29–33] used in this calculation.

Action	Symbol	$L^3 \times T$	a (fm)	m_π (MeV)
DW + ID	24D	$24^3 \times 64$	0.194	139
DW + ID	32Df	$32^3 \times 64$	0.143	143
DW + I	48I	$48^3 \times 96$	0.114	139
DW + I	24I	$24^3 \times 64$	0.111	340
DW + I	64I	$64^3 \times 128$	0.084	139
DW + I	32I	$32^3 \times 64$	0.083	302
$\mathrm{OV}^{0\mathrm{HYP}} + \mathrm{IR}$	JLQCD	$24^3 \times 48$	0.112	290
$\mathrm{HI} + \mathrm{S}^{(1)}$	a12m310	$24^3 \times 64$	0.121	310
$\mathrm{HI} + \mathrm{S}^{(1)}$	a09m310	$32^3 \times 96$	0.088	310
$\mathrm{HI} + \mathrm{S}^{(1)}$	a06m310	$48^3 \times 144$	0.057	310
$\mathrm{HI} + \mathrm{S}^{(1)}$	a04m310	$64^3 \times 192$	0.043	310
$\mathrm{CL}^{\mathrm{stout}} + \mathrm{S}^{\mathrm{tad}}$	C11	$24^3 \times 72$	0.108	290
$\mathrm{CL}^{\mathrm{stout}} + \mathrm{S}^{\mathrm{tad}}$	C08	$32^3 \times 96$	0.080	300
$\mathrm{CL}^{\mathrm{stout}} + \mathrm{S}^{\mathrm{tad}}$	C06	$48^3 \times 144$	0.054	300

the gauge link with smearing parameter 0.125) and tadpole improved Symanzik gauge action at three lattice spacings and $m_\pi \simeq 300$ MeV [32] ($\mathrm{CL}^{\mathrm{stout}} + \mathrm{S}^{\mathrm{tad}}$, $\mathrm{CL}^{\mathrm{stout}}$ for short).

We also repeat the calculation on a JLQCD ensemble [33] at $a = 0.112$ fm and $m_{\pi,\mathrm{ss}} = 290$ MeV. This ensemble uses the 2 + 1 flavor overlap fermion ($\rho = 1.3$ without any HYP smearing [25] on the gauge link) and Iwasaki gauge action with an additional ratio of extra Wilson fermions and associated twisted mass bosonic spinors [34]. The brief information of all the ensembles used in this work is collected in Table I. More details of those ensembles can be found in the Supplemental Material [24].

On the DW/DD ensembles, we use the existing point source DW fermion propagators with the field sparsening compression [35] and generate the valence quark propagators with similar source positions. On the other ensembles, we use the Coulomb gauge fixed wall source to take advantage of the L^3 enhancement of statistics. Note that the wall source using the HISQ action is practically a grid source, which picks only the even points in each spacial direction, as the Dirac space has been mapped to the even/odd sites and should be treated separately in the source. At the same time, we also use low-mode substitution [36] to suppress the statistical uncertainty of the pion correlators using the overlap fermion on the HISQ ensembles at small lattice spacings. The details of the unitary CHROMA [37] + QUDA[38–40] interface for various fermion actions can be found in Ref. [41].

III. RESULTS

The lattice spacing a dependence of $\Delta_{\mathrm{mix,uni}}$ on the DW/DD ensembles are shown in Fig. 1, and the

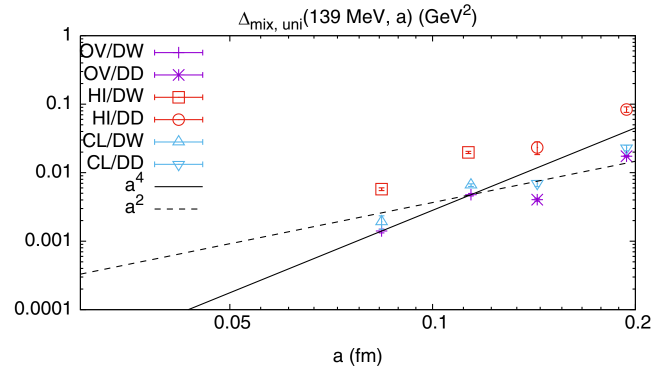

FIG. 1. The mixed-action effect Δ_{mix} on the DW and DD ensembles, as functions of the lattice spacing a. The symbol X/Y means the case with valence fermion action X on the sea fermion action Y. The figure also illustrates the a^4 (solid line) and a^2 (dashed line) dependence for comparison.

symbol X/Y corresponds to the case with valence fermion action X on the sea fermion action Y. If we take $\Delta_{\mathrm{mix}}^{\mathrm{OV/DW}}(a = 0.114\ \mathrm{fm}) = 0.00477(20)\ \mathrm{GeV}^2$ and assume the lattice spacing dependence is a^4 (black line), then the prediction at 0.084 fm will be 0.00141(6), which agrees with the data 0.00141(9) perfectly. On the other hand, the prediction with a simple a^2 dependence (dashed line) will be 0.0026(1), which is more than 5σ higher than the practical result. We can also solve n from the data using the Ca^n form with different valence fermion actions; we obtain $n = 4.0(2)$ (OV/DW, purple crosses), 4.0(2) (HI/DW, red boxes), and 4.0(7) (CL/DW, blue upward triangles), respectively.

It is interesting to see that the similar calculations on two coarse lattice spacings 0.141 and 0.194 fm provide a similar power of the lattice spacing, as $n = 4.8(2)$ (OV/DD, purple stars), 4.2(7) (HI/DD, red circles), and 3.9(4) (CL/DD, blue downward triangles), respectively; but they are a factor ∼2 smaller than $\Delta_{\mathrm{mix}}^{\mathrm{X/DW}}$ assuming an a^4 lattice spacing dependence, as illustrated by the black line for the $\Delta_{\mathrm{mix}}^{\mathrm{OV/DW}}$ case. Such a suppression of Δ_{mix} would relate to the DSDR term, as the setup of the DD and DW ensembles are the same except this term.

Based on the MAPQχPT framework, the quark mass dependence of Δ_{mix} is a NLO correction and is thus relatively weak. It has been verified by our numerical calculations on both the DW + I and $\mathrm{HI} + \mathrm{S}^{(1)}$ ensembles [24]. Thus, we turn to the $\mathrm{HI} + \mathrm{S}^{(1)}$ ensembles [29,30] with ∼310 MeV pion mass to further investigate the lattice spacing dependence of Δ_{mix} with the same simulation setup and show the results in Fig. 2.

With the data at four lattice spacings, it is more obvious that the a^4 behaviors observed on the DW/DD ensembles are not accidental and can dominate in a wide lattice spacing range. Note that the relative uncertainty at $a = 0.043$ fm is large as the mixed-action effect only

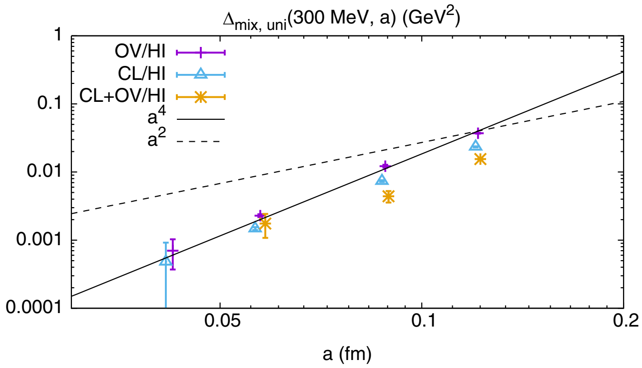

FIG. 2. The mixed-action effects of the overlap fermion (purple crosses) or clover fermion (blue upward triangles) on the HI + $S^{(1)}$ ensembles at four lattice spacings, together with that of the two valence fermion actions (yellow stars). The latter two types of data points are shifted horizontally to improve the visibility.

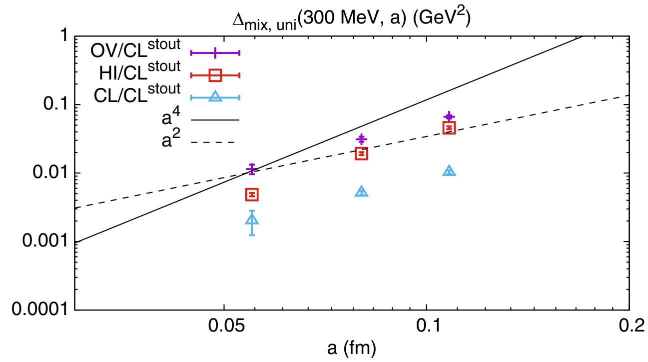

FIG. 3. The mixed-action effects of the overlap fermion (OV, purple crosses), HISQ fermion (HI, red boxes), or HYP smeared clover fermion (CL, blue triangles) on the clover fermion ensembles at three lattice spacings.

changes the pion mass by $\sim 1(1)$ MeV there, and then one cannot exclude the possibility on the dominance of the lower-order lattice spacing dependence [e.g., $\mathcal{O}(a^2)$ as expected by lattice perturbation theory [10]].

We also report the calculation on the $\mathrm{CL}^{\rm stout} + \mathrm{S}^{\rm tad}$ ensembles [32] in the lattice spacing range $a \in [0.054, 0.108]$ fm, and show the results in Fig. 3. Unlike the DW + I or HI + $S^{(1)}$ ensembles using the chiral fermion, $\Delta_{\rm mix,uni}$ at $a = 0.080$ and 0.108 fm look like an a^2 behavior, but the lattice spacing dependence becomes closer to a^4 from $a =$ 0.080 to 0.054 fm. Thus, the behavior at larger lattice spacing could come from the cancellation between the a^4 and a^6 terms. At the same time, the mixed-action effect of the overlap fermion is larger than that of the HISQ fermion, which is also different from the behavior on the DW + I or HI + $S^{(1)}$ ensembles that use the chiral sea fermion actions. Since the $\mathrm{CL}^{\rm stout} + \mathrm{S}^{\rm tad}$ ensembles and HI + $S^{(1)}$ ensembles using similar Symanzik gauge actions with a minor difference in the one-loop correction, the huge $\Delta_{\rm mix,uni}$ would be majorly related to the clover fermion action in the ensembles, while more accurate comparison with exactly the same gauge action is worth further study in the future.

In order to further investigate the likeness between different fermion actions, we define the mixed-action effect of two valence fermion actions B and C on the same gauge ensemble with sea fermion action A as

$$\bar{\Delta}^{\rm B+C/A}_{\rm mix,uni}(m_\pi, a) \equiv m^2_{\pi,\rm BC} - \frac{m^2_{\pi,\rm BB} + m^2_{\pi,\rm CC}}{2}\bigg|_{m_{\pi,\rm BB}=m_{\pi,\rm CC}=m_{\pi,\rm AA}=m_\pi}. \quad (3)$$

As shown in Fig. 2, $\bar{\Delta}^{\rm CL+OV/HI}$ also decreases as a^4 while that at 0.06 fm has large uncertainty. At the same time, we will see that $\bar{\Delta}^{\rm B+C/A}_{\rm mix,uni}$ is very sensitive to the sea action A which does not appear in the definition explicitly.

To make a fair comparison of different cases, we do a linear m_π^2 interpolation based on MAPQχPT and also a linear $\log(a)$ interpolation on $\log \Delta_{\rm mix}(a)$, which is exact when $\Delta_{\rm mix}(a) \propto a^n$. Eventually, we show the interpolated values of $\Delta_{\rm mix,uni}$ and $\bar{\Delta}_{\rm mix,uni}$ on the $\mathrm{OV}^{\rm 0HYP} + \mathrm{IR}$, DW + I, HI + $S^{(1)}$, and $\mathrm{CL}^{\rm stout} + \mathrm{S}^{\rm tad}$ ensembles in Fig. 4, for $a \simeq 0.11$ fm and $m_\pi \in [290, 310]$ MeV.

The red, blue, and purple bars correspond to $\Delta_{\rm mix,uni}$ of the HISQ, clover, and overlap valence fermion actions, respectively. Also, green, orange, and yellow bars correspond to $\bar{\Delta}_{\rm mix,uni}$ of different valence fermion actions. The uncertainties of $\Delta_{\rm mix,uni}$ and $\bar{\Delta}_{\rm mix,uni}$ are also shown at the top of the bar in the figure. In addition, the HISQ valence quark is the same as the sea quark under the HI + $S^{(1)}$

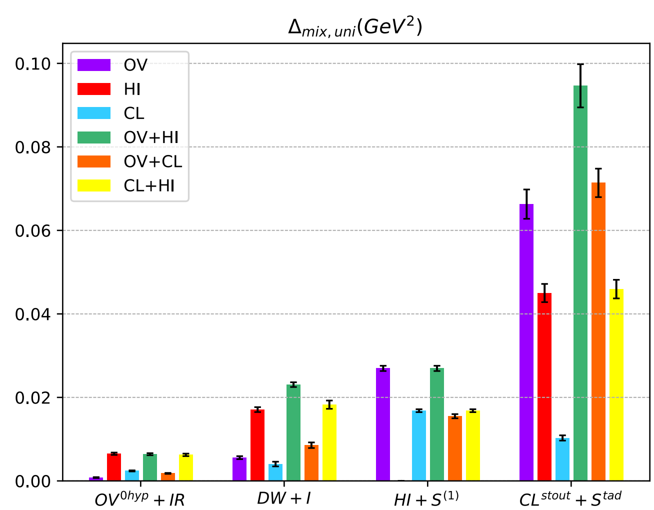

FIG. 4. The mixed-action effects $\Delta_{\rm mix,uni}$ for various valence fermion actions (OV, HI, and CL) and $\bar{\Delta}_{\rm mix,uni}$ for different valence fermion actions (OV + HI, OV + CL, and CL + HI) on the $\mathrm{OV}^{\rm 0HYP} + \mathrm{IR}$, DW + I, HI + $S^{(1)}$, and $\mathrm{CL}^{\rm stout} + \mathrm{S}^{\rm tad}$ ensembles. All the quantities are in units of GeV^2 and are interpolated to $a = 0.11$ fm and $m_\pi \in [290, 310]$ MeV to make a fair comparison.

ensemble, therefore the "HI" bar in the third group of this figure is exactly zero.

From the figure, the mixed-action effect on the $\mathrm{OV}^{0\mathrm{HYP}}+\mathrm{IR}$ ensemble seems to be smaller than the $\mathrm{DW}+\mathrm{I}$ case, which is comparable with the $\mathrm{DW}+\mathrm{ID}$ case given the factor of 2 suppression shown in Fig. 1. It is predictable, as the DSDR term provides somehow similar impact on the near-zero modes of the Dirac operator as the ratio term [34,42].

Compared to the mixed-action effects on the $\mathrm{DW}+\mathrm{I}$ ensembles, those on the $\mathrm{HI}+\mathrm{S}^{(1)}$ ensemble are somehow similar. But when we consider the valence CL or OV action, the $\Delta_{\mathrm{mix,uni}}$ on the $\mathrm{HI}+\mathrm{S}^{(1)}$ ensemble are still larger than those on the $\mathrm{DW}+\mathrm{I}$ ensemble. Since the gauge action used by these two setups are quite different from each other, it requires further study using different fermion actions and the same gauge action to understand the impact of the gauge action in the mixed-action effects.

Contrary to the above three cases, the mixed-action effects on the $\mathrm{CL}^{\mathrm{stout}}+\mathrm{S}^{\mathrm{tad}}$ ensemble are much larger, even for the case of the HYP smeared clover valence fermion action on stout smeared clover sea action. The origin of this huge mixed-action effect presumably relates to the additive chiral symmetry breaking of the clover fermion action.

Besides the sensitivity on the sea actions, our results also suggest that $\bar{\Delta}_{\mathrm{mix,uni}}$ satisfies the following triangle inequalities within the statistical uncertainty,

$$|\Delta^{\mathrm{B/A}}_{\mathrm{mix,uni}}-\Delta^{\mathrm{C/A}}_{\mathrm{mix,uni}}|\le\bar{\Delta}^{\mathrm{B+C/A}}_{\mathrm{mix,uni}}\le\Delta^{\mathrm{B/A}}_{\mathrm{mix,uni}}+\Delta^{\mathrm{C/A}}_{\mathrm{mix,uni}},\qquad(4)$$

$$|\bar{\Delta}^{\mathrm{B+D/A}}_{\mathrm{mix,uni}}-\bar{\Delta}^{\mathrm{C+D/A}}_{\mathrm{mix,uni}}|\le\bar{\Delta}^{\mathrm{B+C/A}}_{\mathrm{mix,uni}}\le\bar{\Delta}^{\mathrm{B+D/A}}_{\mathrm{mix,uni}}+\bar{\Delta}^{\mathrm{C+D/A}}_{\mathrm{mix,uni}},\qquad(5)$$

where D is a valence fermion action different from B and C. The inequalities in Eq. (4) would have fundamental origin other than simple empirical observations, as both the sea action sensitivity and the a^4 behavior of $\bar{\Delta}_{\mathrm{mix,uni}}$ can be deduced from Eq. (5). But MAPQχPT just includes one kind of valence fermion action and should be extended to describe our observations here. The numerical results of $\Delta_{\mathrm{mix,uni}}$ and $\bar{\Delta}_{\mathrm{mix,uni}}$ in all the cases we studied, and also the illustration of Fig. 4 as triangles, can be found in the Supplemental Material [24].

IV. SUMMARY

Based on the calculation of the mixed-action pion mass using three kinds of the fermion actions, including overlap fermion, HISQ fermion, and clover Wilson fermion, on different kinds of the dynamical ensembles, we found that the leading mixed-action effect is numerically small and decreases with small lattice spacing as a^4. It is particularly small when the sea fermion action has chiral symmetry, much smaller than the naive $\mathcal{O}(a^2)$ estimate at small lattice spacings. We note that a similar a^4 behavior was observed in the taste mixing effect of the HISQ fermion in Refs. [4,8].

Based on MAPQχPT, $\Delta_{\mathrm{mix,uni}}$ is the only leading-order low-energy constant, so we expect the mixed-action effect in other quantities will also be $\mathcal{O}(a^4)$, even though this expectation should be verified by the practical calculations. Thus, our study suggests that the "distance" between various discretized fermion actions is closer than the previous estimate, especially at smaller lattice spacings. Furthermore, our observation of the strong sensitivity of $\Delta_{\mathrm{mix,uni}}$ to sea fermion chirality can shed light on a deeper understanding of the impact of chirality in the vacuum on valence quark dynamics.

The result also provides the first quantitative estimate on the systematic uncertainty from the mixed-action lattice QCD simulation and potentially releases the restriction to do the simulation using the gauge ensemble with cheaper fermion actions but larger volume, smaller lattice spacing, and light pion mass. The mixed-action effects studied in this work can also serve as one benchmark for the differences of results obtained with different fermion actions.

ACKNOWLEDGMENTS

We thank the CLQCD, JLQCD, MILC, and RBC/UKQCD Collaborations, for providing us their gauge configurations with dynamical fermions, and Terrence Draper for valuable discussion and comments. The calculations were performed using the CHROMA software suite [37] with QUDA [38–40], GWU code [43,44], and OpenChiral through the HIP programming model [45]. The domain wall propagators were generated using GRID, GPT, and Qlattice. The numerical calculations in this study were carried out on the ORISE Supercomputer and HPC Cluster of ITP-CAS. This research used resources of the Oak Ridge Leadership Computing Facility at the Oak Ridge National Laboratory, which is supported by the Office of Science of the U.S. Department of Energy under Award No. DE-AC05-00OR22725. This work used Stampede time under the Extreme Science and Engineering Discovery Environment (XSEDE), which is supported by National Science Foundation Grant No. ACI-1053575. We also thank the National Energy Research Scientific Computing Center (NERSC) for providing HPC resources that have contributed to the research results reported within this paper. We acknowledge the facilities of the USQCD Collaboration used for this research in part, which are funded by the Office of Science of the U.S. Department of Energy. Y. Y. is supported in part by the Strategic Priority Research Program of Chinese Academy of Sciences, Grants No. XDB34030303 and No. XDPB15, and also the National Natural Science Foundation of China (NSFC) under Grants No. 12047503, No. 12293062. P. S. is supported in part by Strategic Priority Research Program of the Chinese Academy of Sciences under Grant No. XDB34030301. Y. Y. and P. S. are also supported in part by a NSFC-DFG joint grant under Grants No. 12061131006 and No. SCHA 458/22 and the GHfund A No. 202107011598. G. W. is supported by the U.S. DOE Award No. DE-SC0013065, DOE Award No. DE-AC05-06OR23177 which is within the framework of the TMD Topical Collaboration, and the French National Research Agency under the Contract ANR-20-CE31-0016. L. C. J. acknowledges support by DOE Office of Science Early Career Award No. DE-SC0021147 and DOE Award No. DE-SC0010339.

[1] R. Narayanan and H. Neuberger, Nucl. Phys. **B443**, 305 (1995).
[2] H. Neuberger, Phys. Lett. B **417**, 141 (1998).
[3] T.-W. Chiu and S. V. Zenkin, Phys. Rev. D **59**, 074501 (1999).
[4] C. Aubin, T. Blum, M. Golterman, and S. Peris, Phys. Rev. D **106**, 054503 (2022).
[5] Y.-B. Yang, R. S. Sufian, A. Alexandru, T. Draper, M. J. Glatzmaier, K.-F. Liu, and Y. Zhao, Phys. Rev. Lett. **118**, 102001 (2017).
[6] C. C. Chang, A. N. Nicholson, E. Rinaldi, E. Berkowitz, N. Garron, D. A. Brantley, H. Monge-Camacho, C. J. Monahan, C. Bouchard, M. A. Clark *et al.*, Nature (London) **558**, 91 (2018).
[7] Y.-C. Jang, R. Gupta, B. Yoon, and T. Bhattacharya, Phys. Rev. Lett. **124**, 072002 (2020).
[8] S. Borsanyi *et al.*, Nature (London) **593**, 51 (2021).
[9] R. Horsley, H. Perlt, P. E. L. Rakow, G. Schierholz, and A. Schiller (QCDSF Collaboration), Nucl. Phys. **B693**, 3 (2004); **B713**, 601(E) (2005).
[10] O. Bar, G. Rupak, and N. Shoresh, Phys. Rev. D **70**, 034508 (2004).
[11] O. Bar, C. Bernard, G. Rupak, and N. Shoresh, Phys. Rev. D **72**, 054502 (2005).
[12] J.-W. Chen, D. O'Connell, and A. Walker-Loud, J. High Energy Phys. 04 (2009) 090.
[13] G. Wang, J. Liang, T. Draper, K.-F. Liu, and Y.-B. Yang (χQCD Collaboration), Phys. Rev. D **104**, 074502 (2021).
[14] S. Durr, Z. Fodor, C. Hoelbling, S. D. Katz, S. Krieg, T. Kurth, L. Lellouch, T. Lippert, K. K. Szabo, and G. Vulvert, Proc. Sci. LATTICE2007 (**2007**) 115 [arXiv:0710.4769].
[15] K. Orginos and A. Walker-Loud, Phys. Rev. D **77**, 094505 (2008).
[16] C. Aubin, J. Laiho, and R. S. Van de Water, Phys. Rev. D **77**, 114501 (2008).
[17] E. Berkowitz *et al.*, Phys. Rev. D **96**, 054513 (2017).
[18] M. Lujan, A. Alexandru, Y. Chen, T. Draper, W. Freeman, M. Gong, F. X. Lee, A. Li, K. F. Liu, and N. Mathur, Phys. Rev. D **86**, 014501 (2012).
[19] E. Follana, Q. Mason, C. Davies, K. Hornbostel, G. P. Lepage, J. Shigemitsu, H. Trottier, and K. Wong (HPQCD, UKQCD Collaborations), Phys. Rev. D **75**, 054502 (2007).
[20] S. Basak, S. Datta, N. Mathur, A. T. Lytle, P. Majumdar, and M. Padmanath (ILGTI Collaboration), Proc. Sci. LATTICE2014 (**2015**) 083 [arXiv:1412.7248].
[21] P. H. Ginsparg and K. G. Wilson, Phys. Rev. D **25**, 2649 (1982).
[22] T.-W. Chiu, Phys. Rev. D **60**, 034503 (1999).
[23] K.-F. Liu, Int. J. Mod. Phys. A **20**, 7241 (2005).
[24] See Supplemental Material at http://link.aps.org/supplemental/10.1103/PhysRevD.107.L091501 for the discretized fermion and gauge actions used in this paper, and also other mixed-action results not detailed in the main text.
[25] A. Hasenfratz and F. Knechtli, Phys. Rev. D **64**, 034504 (2001).
[26] T. Blum *et al.* (RBC, UKQCD Collaborations), Phys. Rev. D **93**, 074505 (2016).
[27] P. Boyle *et al.*, Phys. Rev. D **93**, 054502 (2016).
[28] A. Hart, G. M. von Hippel, and R. R. Horgan (HPQCD Collaboration), Phys. Rev. D **79**, 074008 (2009).
[29] A. Bazavov *et al.* (MILC Collaboration), Phys. Rev. D **82**, 074501 (2010).
[30] A. Bazavov *et al.* (MILC Collaboration), Phys. Rev. D **87**, 054505 (2013).
[31] A. Bazavov *et al.*, Phys. Rev. D **98**, 074512 (2018).
[32] Q.-A. Zhang, J. Hua, F. Huang, R. Li, Y. Li, C.-D. Lu, P. Sun, W. Sun, W. Wang, and Y.-B. Yang, Chin. Phys. C **46**, 011002 (2022).
[33] H. Fukaya, S. Aoki, T. Chiu, S. Hashimoto, T. Kaneko, J. Noaki, T. Onogi, and N. Yamada (JLQCD, TWQCD Collaborations), Phys. Rev. D **83**, 074501 (2011).
[34] H. Fukaya, S. Hashimoto, K.-I. Ishikawa, T. Kaneko, H. Matsufuru, T. Onogi, and N. Yamada (JLQCD Collaboration), Phys. Rev. D **74**, 094505 (2006).
[35] Y. Li, S.-C. Xia, X. Feng, L.-C. Jin, and C. Liu, Phys. Rev. D **103**, 014514 (2021).
[36] A. Li *et al.* (χQCD Collaboration), Phys. Rev. D **82**, 114501 (2010).
[37] R. G. Edwards and B. Joo (SciDAC, LHPC, UKQCD Collaborations), Nucl. Phys. B, Proc. Suppl. **140**, 832 (2005).
[38] M. A. Clark, R. Babich, K. Barros, R. C. Brower, and C. Rebbi, Comput. Phys. Commun. **181**, 1517 (2010).
[39] R. Babich, M. A. Clark, B. Joo, G. Shi, R. C. Brower, and S. Gottlieb, in Proceeding, SC11 International Conference for High Performance Computing, Networking, Storage and Analysis (2011), arXiv:1109.2935.
[40] M. A. Clark, B. Joó, A. Strelchenko, M. Cheng, A. Gambhir, and R. Brower, arXiv:1612.07873.

[41] K. Zhang, W. Sun, Y.-B. Yang, and R.-Q. Zhang, Proc. Sci. LATTICE2021 (**2022**) 347 [arXiv:2201.09004].
[42] P. M. Vranas, Phys. Rev. D **74**, 034512 (2006).
[43] A. Alexandru, C. Pelissier, B. Gamari, and F. Lee, J. Comput. Phys. **231**, 1866 (2012).
[44] A. Alexandru, M. Lujan, C. Pelissier, B. Gamari, and F. X. Lee, in *Proceedings, 2011 Symposium on Application Accelerators in High-Performance Computing (SAAHPC'11): Knoxville, Tennessee, July 19-20, 2011* (2011), pp. 123–130, arXiv:1106.4964.
[45] Y.-J. Bi, Y. Xiao, W.-Y. Guo, M. Gong, P. Sun, S. Xu, and Y.-B. Yang, Proc. Sci. LATTICE2019 (**2020**) 286 [arXiv:2001.05706].